Int J Adv Manuf Technol (2010) 47:535–542
DOI 10.1007/s00170-009-2230-5

ORIGINAL ARTICLE

Analysis of directional factors in milling: importance of multi-frequency calculation and of the inclusion of the effect of the helix angle

Mikel Zatarain · Iñigo Bediaga · Jokin Muñoa · Tamás Insperger

Received: 14 September 2008 / Accepted: 20 July 2009 / Published online: 16 August 2009

Abstract The concept of directional factor for chatter stability analysis has been used from a long time ago. The analysis of its evolution for different feed directions in milling processes provides a good way of selecting the best cutting conditions. For very stable cutting directions, corresponding to very low directional factors, the single frequency analysis gives unacceptable results and multi-frequency, or alternative solutions as semi-discretisation must be used. It is found also that the period doubling lobes extend at both sides of the tooth pass frequency equivalent to twice the natural frequency. In these cases, helix angle has a very important effect on the stability. For end milling processes, where the mill axial pitch can be of the order of the stable limit depth of cut, a very stable situation is found except in those areas corresponding to period doubling, where instability islands are found. Besides, a graphical construction for accurate estimation of the stable limit depth of cut and starting rotational speed of the period doubling lobes is proposed.

Keywords Milling · Stability · Dynamics

1 Introduction

The first theories explaining the uprising of chatter as a regenerative phenomenon were developed by Tobias and Fishwick [1] and by Tlusty and Polacek [2]. Later, Merrit [3] interpreted the system as a feedback process, what simplified the understanding. Since those days, the concept of directional factor was used as a way to quantify the projections of cutting force to mode direction and of mode direction to chip thickness.

For milling processes, where these geometrical projections vary constantly, Opitz [4] and Tlusty [5] proposed two alternative ways of calculating 'equivalent' directional factors. By means of them, limit depth of cut diagrams for milling, for one degree of freedom systems, could be obtained.

Much more recently, Altintas and Budak [6] showed the way of obtaining the lobe diagrams for milling processes for systems with two or even three degrees of freedom. In this case, they worked on a Cartesian base and did not use the concept of directional factors. Instead, they used a directional matrix, which is more difficult to be interpreted. This directional matrix was developed in a Fourier series in the harmonics of the rotation frequency. The system was simplified by considering the zero order term of the Fourier series only.

Later, Budak and Altintas [7] developed the solution for obtaining the lobe diagram of milling processes including more than one term of the Fourier series development. This approach gives rise to the so-called multi-frequency solution, in which chatter vibration has several frequency components separated by the cutting frequency.

Other developments by Davies et al. [8], Insperger and Stépán [9, 10] and Bayly et al. [11] obtained the stability limits using different methods in the time domain, by separating the solution between the forced part and the stability problem, giving rise to an eigenvalue system. These methods showed that in milling with low radial immersion new instability areas, period doubling or flip

M. Zatarain · I. Bediaga (✉) · J. Muñoa
Ideko IK4 Technological Centre,
Elgoibar, Spain
e-mail: ibediaga@ideko.es

T. Insperger
Department of Applied Mechanics, Budapest
University of Technology and Economics,
Budapest, Hungary

lobes appear. Later, Merdol and Altintas [12] showed that the multi-frequency solution can also be used in order to obtain the period doubling instability.

By using the multi-frequency approach, Zatarain et al. [13] showed that the helix of the tool produces the transformation of the added lobes into instability islands. Insperger et al. [14] arrived to the same conclusion by using the semi-discretisation method.

All these modern developments have forgotten the concept of directional factor. Indeed, they all, or almost all of them, considered systems with modal displacements parallel to one of the coordinate axes. For modes coming from the deformation of the tool or of the main spindle, this approach seems reasonable, but for structural modes, it is not possible to accept such a simplification.

Lobe diagrams for milling with modes in directions not parallel to the Cartesian axes could be obtained by using directional matrices, but an approach by means of directional factors is more natural and intuitive. Indeed, it gives the possibility of easily estimating stable limit depths of cut without the need of using computers and specially developed software systems.

2 Directional factors in time independent systems

In a time-invariant system with a single mode, like the turning process shown in Fig. 1, the effect of the cutting force on the modal displacement is obtained by including the cosines of the angle between force and mode direction,

$$\left(\ddot{q} + 2 \times \zeta \times \omega_n \times \dot{q} + \omega_n^2 \times q\right) = \phi \times f \times \cos\alpha \tag{1}$$

where q is the modal participation (displacement), ω_n and ζ are, respectively, the natural frequency and damping ratio, ϕ is the tool-work relative mode amplitude for a unit modal mass, f is cutting force and α is the angle between force and mode displacement direction.

The chip thickness is obtained by adding up the static chip thickness, due to the feed per revolution, with the dynamic component coming from the modal displacement. The static component gives rise to a constant force, which does not influence the dynamic stability. As a consequence, it is possible to consider only the dynamic component, which is calculated by including the current and the previous revolution displacements,

$$h = -\phi \times (q(t) - q(t-\tau)) \times \cos\beta \tag{2}$$

where β is the angle of the mode displacement and the chip thickness directions.

The dynamic component of the cutting force is obtained by multiplying the dynamic chip thickness by the cutting coefficients,

$$\{f\} = \begin{Bmatrix} k_t \\ k_r \\ k_a \end{Bmatrix} b \times h = k_t \times \begin{Bmatrix} 1 \\ \rho_r \\ \rho_a \end{Bmatrix} \times b \times h$$
$$= k_c \times \begin{Bmatrix} r_t \\ r_r \\ r_a \end{Bmatrix} \times b \times h \tag{3}$$

In Eq. 3, two different alternatives are proposed: that of using the tangential cutting force coefficient k_t and that of using the total force coefficient k_c. The choice of one or the other has a direct influence on the values of the directional factors that will be obtained, but of course, the final result is unaffected.

Combining Eqs. 1, 2 and 3

$$\begin{aligned} &\left(\ddot{q} + 2 \times \zeta \times \omega_n \times \dot{q} + \omega_n^2 \times q\right) \\ &\quad = -\phi^2 \times b \times k_c \times \psi_c \times (q(t) - q(t-\tau)) \\ &\quad = -\phi^2 \times b \times k_t \times \psi_t \times (q(t) - q(t-\tau)) \\ &\psi_c = \cos\alpha \times \cos\beta \equiv \text{directional factor based on } k_c \\ &\psi_t = \cos\alpha \times \cos\beta / r_t \equiv \text{directional factor based on } k_t \end{aligned} \tag{4}$$

In Eq. 4, directional factor was defined as the product of the cosines of the angles, α, between cutting force and modal direction and β between modal direction and chip thickness direction, as shown in Fig. 1.

Applying the Laplace transform to Eq. 4, and taking into consideration that $\phi^2 = 1/m$, m being the mass reduced to the modal relative displacement between tool and workpiece:

$$\begin{aligned} &m \times \left(s^2 + 2 \times \zeta \times \omega_n \times s + \omega_n^2\right) \times Q \\ &\quad = -b \times k_c \times \psi_c \times Q \times (1 - e^{-s \times \tau}) \end{aligned} \tag{5}$$

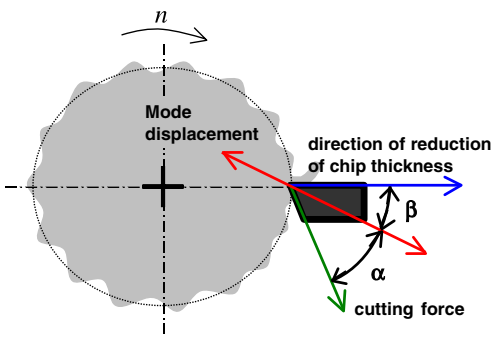

Fig. 1 Cutting force and mode and chip directions

The stability lobe diagram is obtained by solving Eq. 5 to obtain pure imaginary solutions for the Laplace variable s. For that, we substitute s by $j\omega$, and operating:

$$b = \frac{-1}{2 \times k_c \times \psi_c \times R} \tag{6}$$

where R is the real part of the transfer function

$$\frac{\Delta}{F} = \frac{1}{m \times \left(s^2 + 2 \times \zeta \times \omega_n \times s + \omega_n^2\right)} \tag{7}$$

From Eq. 6, it is clear that, provided that the directional factor is positive, the real part of the transfer function must be negative for the limit depth to be a positive value. That means that the lobes will start at the condition where the vibration frequency gives rise to real part of transfer function equal to zero, for which the limit depth is infinite, and then continue through the left part of the Nyquist diagram, that is, higher vibration frequencies. The corresponding rotation frequency is obtained by the equation:

$$\tan\left(\frac{\omega \times \tau}{2}\right) = \frac{I}{R} \tag{8}$$

where R and I are the real and imaginary parts of the transfer function, ω is the vibration frequency and τ is the period of the rotation, inverse of the frequency in Hz.

It is well known that the absolute minimum stable depth of cut is obtained for the vibration frequency that produces the maximum negative value of the real part of the transfer function. For small damping factors, which are the general cases in machine tools so that frequency can accurately be estimated by

$$\omega = \omega_n \times (1 + \zeta) \tag{9}$$

and the value of the real part is:

$$R = \frac{-1}{4 \times k \times \zeta \times (1 + \zeta)} \tag{10}$$

where k is the stiffness of the mode reduced to the relative displacement between tool and part.

As a consequence, the absolute minimum stable depth of cut is

$$b = \frac{2 \times k \times \zeta \times (1 + \zeta)}{k_c \times \psi_c} \tag{11}$$

2.1 Evolution of directional factors with mode direction

From Fig. 1, it becomes clear that for different mode directions, the value of the directional factor will be different. Figure 2 shows this evolution. Whenever the mode is perpendicular to the resultant cutting force, or to the chip thickness direction, the directional factor will null.

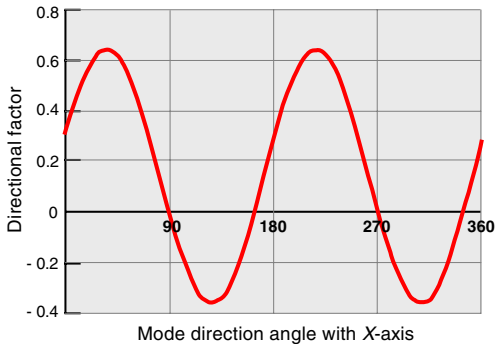

Fig. 2 Dependency of directional factor with mode direction

For some mode directions, the directional factor will become negative (see Fig. 2). It is possible to understand negative directional factors as cases in which the cutting force produces a mode displacement tending to further penetration of the tool into the workpiece. Positive directional factors mean that the cutting force tends to produce separation of the tool from the workpiece.

As the absolute limit depth of cut is inversely proportional to the directional factor, situations with very small directional factors will produce very stable processes.

2.2 Adimensional lobe diagrams

For single-mode systems, it is possible to work with adimensional lobe diagrams, by normalising the rotation frequency by the natural frequency, and the limit depth of cut by the product $2 \times k \times \zeta \times (1 + \zeta)/k_c \times \psi_c$ where k is the stiffness of the mode, equal to $m \times \omega_n^2$. In this way, the diagrams only differ when damping is changed, and the absolute limit depth of cut is always 1. Figure 3a shows the lobes diagram for a system with positive directional factor. Figure 3b shows the zero-order lobe for three different values of damping ratios.

As was shown before, directional factors can have negative values, whenever the projection of the cutting force on the mode direction produces an increase in chip thickness, that is, when the cutting force produces penetration of the tool into the workpiece. This is not an uncommon case, but it seems that it has been paid very little attention in the bibliography.

Negative directional factors produce a change in the frequency range at which chatter can arise. In this case, chatter frequencies are lower than the natural frequency. Figure 4a shows the lobe diagram of a system with negative directional factors, and Fig. 4b shows the zero-order lobe for different values of damping ratio.

It is interesting to note that by calculating the directional factor, it is possible to exactly obtain the absolute minimum limit depth of cut, both for positive and negative factors.

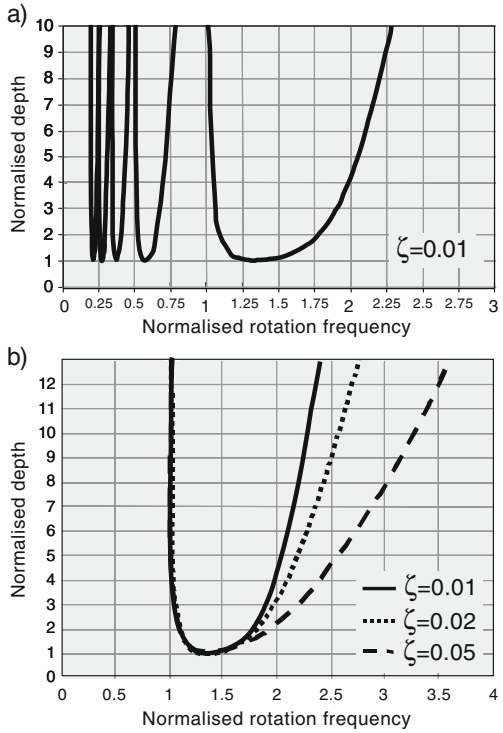

Fig. 3 Adimensional stability diagram for positive directional factor (**a**) and three different damping ratios (**b**)

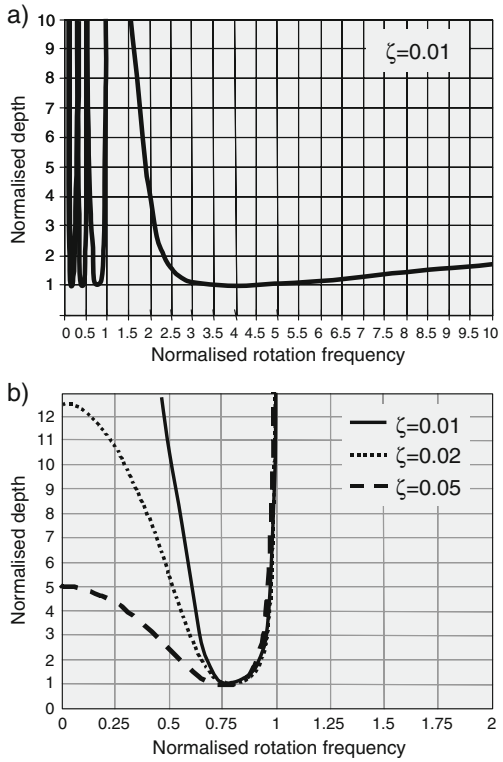

Fig. 4 Adimensional stability diagram for negative directional factor (**a**) and three different damping ratios (**b**)

3 Directional factor for milling processes

Milling processes are characterised by the variation of the geometry of the process as the tool rotates, as shown in Fig. 5. That gives rise to a much more difficult problem to solve than that of continuous processes like turning.

The extrapolation of the equation of limit stable depth of cut for continuous processes to the discontinuous process of milling should consider the proportion of time in cut to the total time and also the number of teeth of the mill. The transformed equation could be written as:

$$b = \frac{-1}{2 \times k_c \times \psi_c \times \frac{\Delta\upsilon}{2\times\pi} \times z \times R} \tag{12}$$

where $\Delta\upsilon$ is the arc in cut (angular distance between start angle and exit angle), and z is the number of teeth of the tool.

As in milling processes, the directions of the cutting force and of the chip thickness change constantly, also the value of the directional factor changes. Opitz [4] proposed to use the average of the directional factor in the cutting arc:

$$\psi_{av} = \frac{1}{\upsilon_{ex} - \upsilon_{st}} \int_{\upsilon_{st}}^{ex} \psi \times d\upsilon \tag{13}$$

Later, Tlusty [5] proposed to use the geometric mean of the directional factor, or in other words, calculate the directional factor for the middle of the immersion:

$$\upsilon_0 = \frac{\upsilon_{st} + \upsilon_{ex}}{2} \tag{14}$$

Altintas et al. [6] and Budak et al. [7] showed that the milling process can accurately be modelled by using a Fourier expansion of a directional matrix. For large angular immersions, the first term of the expansion gives suffi-

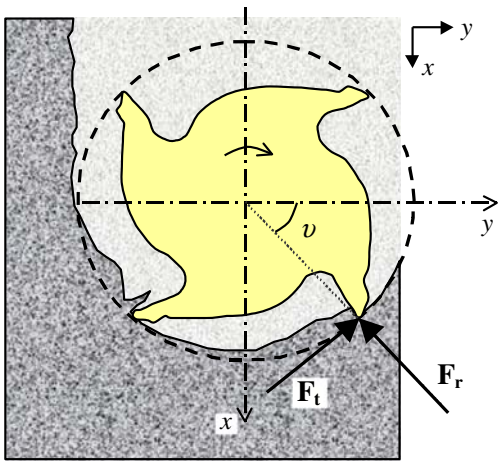

Fig. 5 Cutting force in milling process

ciently accurate results, and it coincides exactly with the approximation proposed by Opitz [4].

3.1 Repetitive impact-driven chatter

When angular immersion is small, additional stability lobes appear, producing an increase of stability in a small area and a reduction in a larger area [8–12]. For the main flip lobe, only harmonics 0 and −1 are relevant, and they both have equal amplitude and different phase. The resulting equation is

$$\begin{Bmatrix} Q_{-1} \\ Q_0 \end{Bmatrix} = -b \times k_c \times \left(1 - e^{-j\times\omega\times\tau}\right) \times \begin{bmatrix} \psi_0 \times H_{-1} & \psi_{-1} \times H_0 \\ \psi_1 \times H_{-1} & \psi_0 \times H_0 \end{bmatrix} \begin{Bmatrix} Q_{-1} \\ Q_0 \end{Bmatrix} \quad (15)$$

where H_0 and H_{-1} are, respectively, the transfer functions at frequencies ω and $\omega-\omega$, while $\psi_0\ \psi_1\ \psi_{-1}$ are the harmonics of the directional factor.

Taking into account that at flip situation $\Omega = 2 \times \omega$, then $1 - e^{-j\times\omega\times\tau} = 1 - e^{-j\times\omega\times\frac{2\times\pi}{2\times\omega}} = 1 - e^{-j\times\pi} = 2$, so

$$\begin{Bmatrix} Q_{-1} \\ Q_0 \end{Bmatrix} = -2 \times b \times k_c \times \begin{bmatrix} \psi_0 \times H_{-1} & \psi_{-1} \times H_0 \\ \psi_1 \times H_{-1} & \psi_0 \times H_0 \end{bmatrix} \begin{Bmatrix} Q_{-1} \\ Q_0 \end{Bmatrix} \quad (16)$$

Also, $H_{-1} = H(-j \times \omega) = H * (j \times \omega) = H_0^* = H*$, and $\psi_{-1} = \psi_1^*$, where * indicates complex conjugate. Working out, the eigenvalue problem to be solved becomes

$$\begin{bmatrix} \psi_0 \times H * +\lambda & \psi_1^* \times H \\ \psi_1 \times H* & \psi_0 \times H + \lambda \end{bmatrix} \begin{Bmatrix} Q_{-1} \\ Q_0 \end{Bmatrix} = 0 \quad (17)$$

$\lambda = \frac{1}{2\times b\times k_s}$

The eigenvalues of the matrix are

$$\lambda = -\psi_0 \times R \pm \sqrt{\psi_0^2 \times R^2 - \left(\psi_0^2 - |\psi_1|^2\right) \times |H|^2} = = -\psi_0 \times R \pm \sqrt{|\psi_1|^2 \times |H|^2 - \psi_0^2 \times I^2} \quad (18)$$

where R, I, are, respectively, the real and imaginary parts of the frequency response function.

For the eigenvalues to take real values, the following must be fulfilled:

$$|\psi_1|^2 \times |H|^2 - \psi_0^2 \times I^2 \geq 0 \quad (19)$$

or

$$\frac{I^2}{|H|^2} \leq \frac{|\psi_1|^2}{\psi_0^2} \quad (20)$$

Whenever the magnitude of the harmonic 1 of the directional factor is lower than that of harmonic 0, the meaning of Eq. 20 can be appreciated in Fig. 6. The red circle-like curve represents the Nyquist plot of the frequency response function (FRF). The vectors ψ_0 and ψ_1 represent the harmonics 0 and 1 of the Fourier development of the directional factor. The harmonic 1 is represented in vertical, while the harmonic 0 is represented at an angle such that its vertical projection equals the length of the first harmonic. Then, the intersection of this vector with the FRF indicates the vibration frequency at which period doubling lobe will start.

From Fig. 6, it follows that for flip bifurcation to occur, the vibration frequency must be larger than the limit frequency defined by the dotted blue vector. In milling as in turning, the directional factor can be negative. In that case, period doubling limit is at the other side of the imaginary axis, and the chatter frequency will be lower than the limit frequency defined by the dashed green line. As a comparison, Hopf lobes start at exactly –π/2, corresponding exactly to the natural frequency. For illustration purposes, a system with the following parameters will be considered:

- Machine/part/tool dynamic parameters: natural frequency 319.4 Hz, damping ratio 0.0196, stiffness 21.6 N/μm, mode direction parallel to X-axis.
- Process parameters: end mill, diameter 20 mm, four flutes, helix angle 30º corresponding to 27 mm axial pitch, tangential cutting pressure 713.12 N/mm^2, radial to tangential ratio 0.21, axial to tangential ratio −0.279; radial immersion 50% of diameter of tool.

Figure 7 shows the evolution of harmonic 0 and of the magnitude of harmonics 1 and 3 for these parameters for variable angle between feed direction and X-axis.

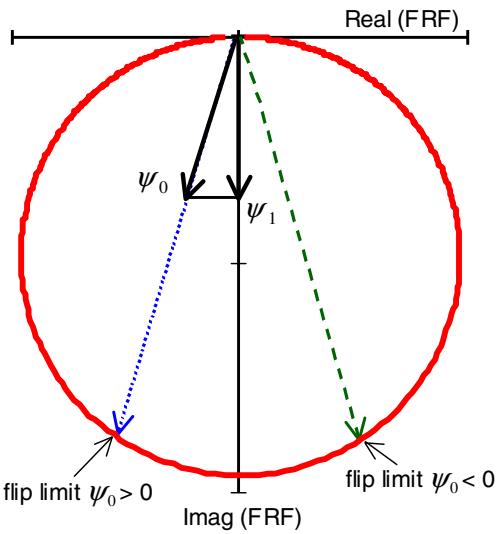

Fig. 6 Starting frequency for period doubling chatter

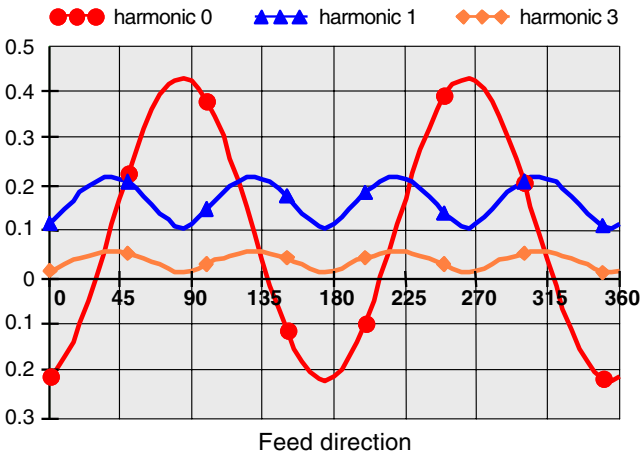

Fig. 7 Harmonics of directional factor

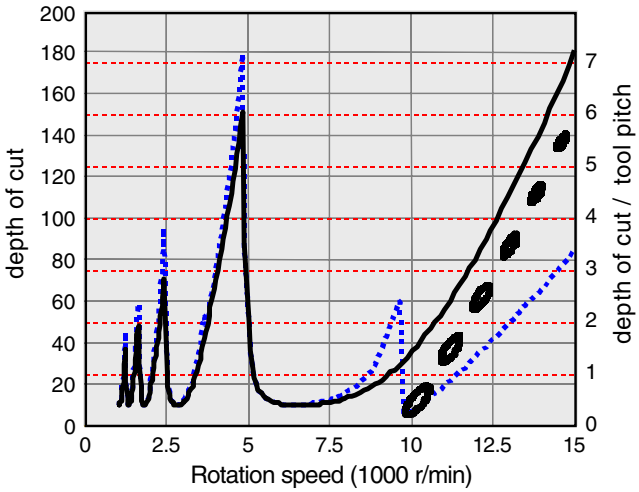

Fig. 9 Stability limits for straight and helical mills

4 Influence of helix angle of tool on flip lobes

Zatarain et al. [13] and Insperger et al. [14] showed that the helix angle is an important issue when analysing period doubling lobes. It was shown [13] that the helix gives rise to a reduction of the ψ_1 harmonics and subsequent of the directional factor. That produces the change of the flip lobes into instability islands. The factor of reduction for the first harmonic is

$$g_1 = \frac{1 - e^{-j\times\frac{2\times\pi\times b}{p}}}{j\times\frac{2\times\pi}{p}} \tag{21}$$

which is represented in Fig. 8.

Figure 9 shows in black the stability limit for helical mill, where the islands are unstable closed areas inside a stable region. For comparison, the dotted blue line shows the stability limit for the same conditions except mill was considered non helical. It becomes clear that flip does not appear for depths of cut equal to multiples of the tool axial pitch.

4.1 Lobe diagrams for very small harmonic 0

The condition that the harmonic 1 of the Fourier development of the directional factor should be smaller than the harmonic 0 is not always satisfied. Varying the feed direction, provided that the passive force coefficients are not extremely large, the value of harmonic 0 will null for some directions. On the contrary, as shown in Fig. 7, the magnitude of harmonic 1 has smaller variations with the feed direction, and as a consequence, it is possible that it takes larger values than the value for harmonic 0.

If Eq. 9, obtained considering only the harmonic 0, is applied to the frequency with the most negative real part, the absolute limit depth of cut is obtained:

$$b_{\text{limit}} = \frac{2\times k\times\zeta\times(1+\zeta)}{\psi_0\times z\times k_t\times\frac{\Delta v}{2\times\pi}} \tag{22}$$

The evolution of the limit calculated from Eq. 22 for different feed directions is shown in Fig. 10

The lobe diagrams calculated by the single frequency solution for feed directions 0º, 30º and 90º are shown in

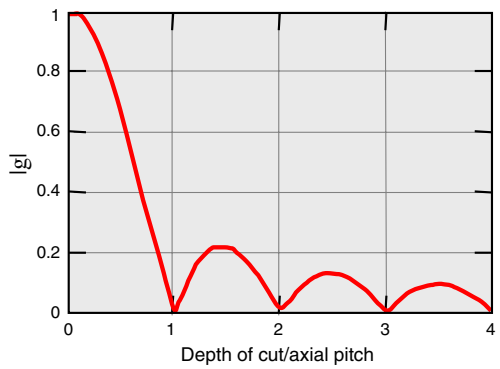

Fig. 8 Reducing factor due to helix angle

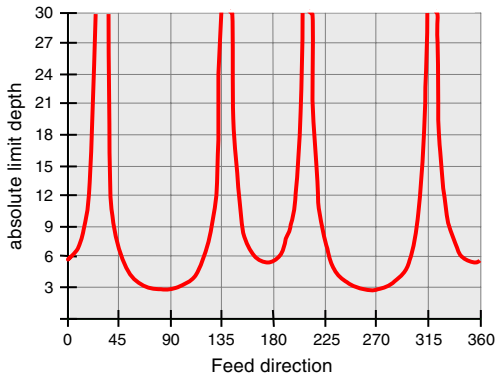

Fig. 10 Evolution of absolute limit depth of cut

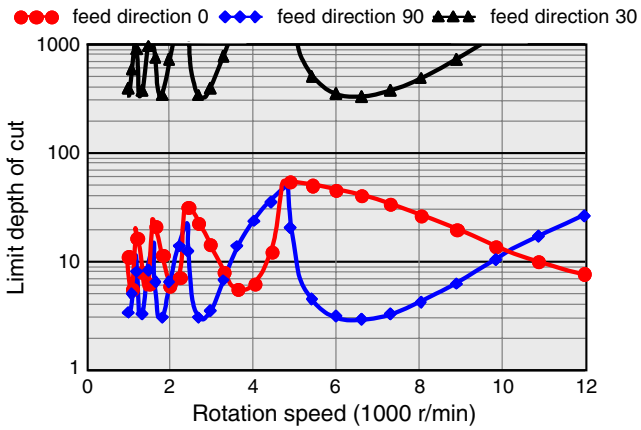

Fig. 11 Lobe diagrams for different feed directions obtained by single frequency calculation

Fig. 11. The diagram is in semi-logarithmic scale because the limits for feed at 30º are extremely high. The absolute stability limits obtained are exactly equal to the limits calculated by Eq. 22. For feed direction 30º the directional factor is almost null, producing a very stable situation if the single frequency calculation is used.

Figure 12 shows the lobe diagrams for the same conditions except feed directions are 30º, 28º and 32º, illustrating the behaviour for small directional factors.

Coming back to Eq. 20, it becomes clear that when harmonic 1 of the directional factor is larger than harmonic 0 period doubling chatter is not limited to one or the other side of the natural frequency. Working out Eq. 17 for values of harmonic 1 larger than harmonic 0 produces the absolute limit depth of cut due to flip instability:

$$b_{\text{flip}} = \frac{k \times \zeta}{\sqrt{|\psi_1|^2 - \psi_0^2} \times z \times k_t \times \frac{\Delta\upsilon}{2\times\pi}} \text{ if } |\psi_1| > |\psi_0| \qquad (23)$$

Figure 13 shows absolute limits calculated after Eq. 22 for Hopf lobes and after Eq. 23 for flip lobes. This latter

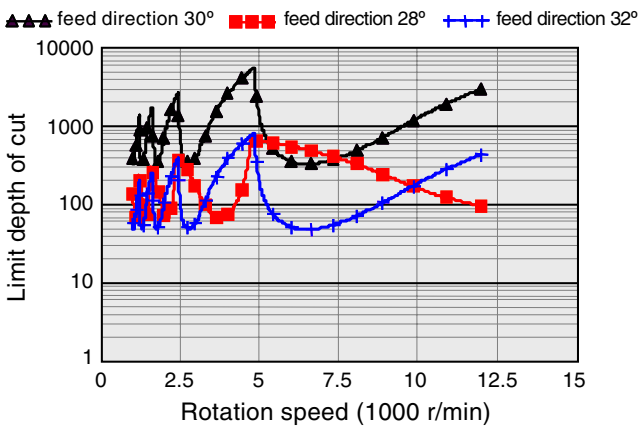

Fig. 12 Lobe diagrams for feed directions close to the one with directional factor equal to zero

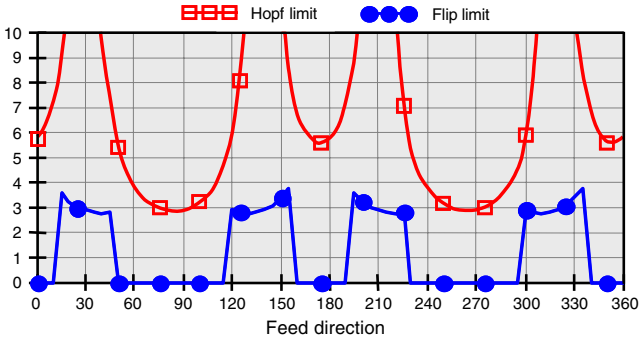

Fig. 13 Absolute limit depth of cut (mm) estimated after Eqs. 22 and 23

was only applied for the feed directions producing a harmonic 1 with larger magnitude than harmonic 0.

From Fig. 13, it is followed that in many instances, flip absolute limit will take much lower values than Hopf limits. The lobe diagram for the feed direction 30º, which is very favourable from the point of view of the Hopf instability, is shown in Fig. 14. Dashed blue line corresponds to a straight mill, while the continuous black islands are the instability limits for the helical mill with axial pitch 27 mm. Semi-logarithmic scale is applied again, because of the very high limit depths for the helical mill.

It is interesting to remark that Fig. 14 was obtained with the same data used for Fig. 11 for feed direction 30º. The only difference was that multi-frequency was applied rather than single-frequency approach. The diagrams were validated by the semi-discretisation method, which produced very similar results.

If the mill is straight, or has a very long axial pitch, the stability limit calculated by single-frequency approach is enormously larger than when multi-frequency is applied,

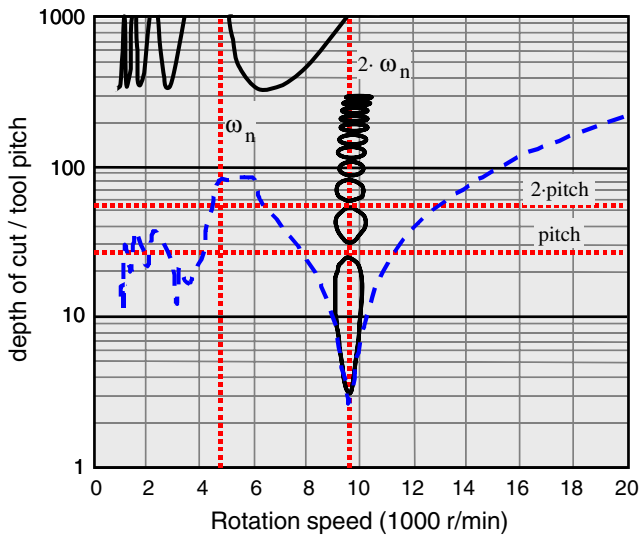

Fig. 14 Stability lobes for helical mills (*black line*) and straight mills (*dashed blue line*)

which should be considered the exact solution. In this example, the limit depth calculated by single frequency was 325 mm, while by multi-frequency is 2.85 mm, with limits for other speeds than the worst in the range of 10 mm.

But when the mill is helical, and the helix is taken into consideration in the calculation, the reduction of stability by inclusion of the harmonics of the directional factor is only important for cutting frequencies close to twice the natural frequency. In this region, the low stability of 2.85 mm is maintained, whereas for the other speeds the limit obtained by single-frequency approach is correct.

It becomes evident that in the situations when the harmonic 0 of the directional factor becomes small, flip instability produces a very important reduction of the stability, even with large radial mill immersions.

5 Conclusions

From the analysis carried out, it can be concluded that the harmonic 0 of the directional factor provides a good way to characterise the best feed directions for milling.

Nevertheless, there could be some special situations. In the literature, the situations with negative directional factors have been paid very low attention. It was shown in this paper that in processes giving rise to this situation, the shape of the stability limit lobes is completely changed.

Moreover, the period doubling instability arises for low radial immersion milling. In this research, a simple equation for calculating the absolute stable limit depth of cut at flip situation is proposed, and also, a graphical construction for obtaining the starting frequency of flip chatter, both for positive and negative directional factors, is detailed.

In some circumstances, for particular feed directions, the harmonic 0 of the directional factor becomes very small. In this case, the harmonic 1 controls the lobe diagram, producing lobe diagrams with shape different to the usual. Flip lobes are not limited to one or to the other side of the natural frequency but extend to both sides. These lobes take a pronounced V-shape, different to the usual shape of flip lobes, and limit the stability for a large part of the cutting frequencies.

However, when the mill is helical and its axial pitch is not much larger than the stability limit depth of cut, the reduction of stable depth only arises at the flip cutting frequency, around twice the natural frequency.

References

1. Tobias SA, Fiswick W (1958) Theory of regenerative machine tool chatter. The Engineer, London
2. Tlusty J, Polacek M (1957) Beispiele der behandlung der selbsterregten Schwingung der Werkzeugmaschinen FoKoMa. Hanser Verlag, Munich
3. Merrit H (1965) Theory of self-excited machine tool chatter. Transactions of the ASME, Journal of Engineering for Industry 87:447–454
4. Opitz H (1969) Investigation and calculation of the chatter behavior of lathes and milling machines. CIRP Ann 18:335–342
5. Altintas Y, Weck M (2004) Chatter stability of metal cutting and grinding. CIRP Ann 53:619–642
6. Altintas Y, Budak E (1995) Analytical prediction of stability lobes in milling. CIRP Ann 44:357–362
7. Budak E, Altintas Y (1998) Analytical Prediction of Chatter Stability Conditions for Multidegree of Freedom Systems in Milling. Part I: General Formulation, Part II: Application of the General formulation to Common Milling Systems. Transactions of the ASME, Journal of Engineering for Industry 120:22–36
8. Davies M, Pratt JR, Dutterer BS, Burns TJ (2000) The stability of low radial immersion milling. CIRP Ann 49:37–40
9. Insperger T., Stépán G., (2000) Stability of High Speed Milling. In Proceedings of the ASME International Engineering Congress and Exposition, Orlando, Florida, pp. 119-123
10. Insperger T, Stépán G (2004) Updated semi-discretization method for periodic delay-differential equations with discrete delay. International Journal of Numerical Methods in Engineering 61:117–141
11. Bayly PV, Halley JE, Mann BP, Davies MA (2003) Stability of interrupted cutting by temporal finite element analysis. International Journal of Manufacturing Science and Engineering 125:220–225
12. Merdol SD, Altintas Y (2004) Multi frequency solution of chatter stability for low immersion milling. J Manuf Sci Eng 126:459–466
13. Zatarain M, Muñoa J, Peigné G, Insperger T (2006) Analysis of the influence of mill helix angle on chatter stability. CIRP Ann 55 (1):365–368
14. Insperger T, Muñoa J, Zatarain M, Peigné G (2006) Unstable Islands in the Stability Chart of Milling Processes Due to the Helix Angle. CIRP 2nd International Conference on High Performance Cutting, Vancouver, Canada, pp 12–13